



LAWRENCE
LIVERMORE
NATIONAL
LABORATORY

Nature of the Pygmy Resonance in Continuous Gamma-Spectra

A. Voinov, A. Schiller, E. Algin, L.A. Bernstein, P.E.
Garrett, M. Guttormsen, J. Rekstad, S. Siem, R.O.
Nelson

December 4, 2003

Meetings in Bogoliubov Laboratory of Theoretical Physics
Dubna, Russia
September 2, 2003 through September 6, 2003

Disclaimer

This document was prepared as an account of work sponsored by an agency of the United States Government. Neither the United States Government nor the University of California nor any of their employees, makes any warranty, express or implied, or assumes any legal liability or responsibility for the accuracy, completeness, or usefulness of any information, apparatus, product, or process disclosed, or represents that its use would not infringe privately owned rights. Reference herein to any specific commercial product, process, or service by trade name, trademark, manufacturer, or otherwise, does not necessarily constitute or imply its endorsement, recommendation, or favoring by the United States Government or the University of California. The views and opinions of authors expressed herein do not necessarily state or reflect those of the United States Government or the University of California, and shall not be used for advertising or product endorsement purposes.

Nature of the pygmy resonance in continuous γ -spectra

A. Voinov,^{1,*} A. Schiller,² E. Algin,^{2,3,4,5} L.A. Bernstein,² P.E. Garrett,²
M. Guttormsen,⁶ R.O. Nelson,⁷ J. Rekstad,⁶ and S. Siem⁶

¹*Frank Laboratory of Neutron Physics, Joint Institute of Nuclear Research,
141980 Dubna, Moscow region, Russia*

²*Lawrence Livermore National Laboratory, L-414,
7000 East Avenue, Livermore, California 94551*

³*North Carolina State University, Raleigh, North Carolina 27695*

⁴*Triangle Universities Nuclear Laboratory, Durham, North Carolina 27708*

⁵*Department of Physics, Osmangazi University, Meselik, Eskisehir, 26480 Turkey*

⁶*Department of Physics, University of Oslo, N-0316 Oslo, Norway*

⁷*Los Alamos National Laboratory, H-855,
Bikini Atoll Road, Los Alamos, New Mexico 87545*

Two-step-cascade spectra of the $^{171}\text{Yb}(n, \gamma\gamma)^{172}\text{Yb}$ reaction have been measured using thermal neutrons. They are compared to calculations based on experimental values of the level density and radiative strength function obtained from the $^{173}\text{Yb}({}^3\text{He}, \alpha\gamma)^{172}\text{Yb}$ reaction. The multipolarity of a $6.5(15) \mu_N^2$ resonance at $3.3(1)$ MeV in the strength function is determined to be $M1$ by this comparison.

PACS numbers: 25.40.Lw, 25.20.Lj, 24.30.Gd, 27.70.+q

Excited nuclei decay often by a cascade of γ rays. While the decay between discrete states is determined by the details of the nuclear wavefunctions, unresolved transitions are best described by statistical concepts like a continuous radiative strength function (RSF) and level density. The RSF (reviewed in [1]) provides the mean value of the decay probability for a given γ -ray energy E_γ . For hard γ rays, (~ 7 – 20 MeV), the RSF is governed by the giant electric dipole resonance whose parameters are determined from photoabsorption [2]. The soft tail of the RSF has been investigated by a variety of methods, most notably by primary γ rays [3]. Recently, systematic studies of the soft RSF have been performed at

*Electronic address: voinov@nf.jinr.ru

the Oslo Cyclotron Laboratory using a method based on sequential extraction. With this method it is possible to obtain both the level density and RSF by a deconvolution of a set of primary γ spectra from a range of excitation energies [4]. Total RSFs (summed over all multipolarities) of rare earth nuclei can be extracted for $B_n > E_\gamma > 1$ MeV [5]. Their common, most striking feature is a resonance at $E_\gamma \sim 3$ MeV which is believed to be of dipole multipolarity but whose electromagnetic character is unknown. It has been shown for all investigated rare earth nuclei that the total RSF is most readily decomposed into a sum of the Kadenskii-Markushev-Furman (KMF) $E1$ model [6], a spin-flip $M1$ model [7], and the aforementioned soft dipole resonance [5]. The knowledge of the character of this resonance is essential for its theoretical interpretation. Experimentally, it can be determined from an auxiliary two-step-cascade (TSC) measurement [8].

The TSC method is based on the observation of decays from an initial state i to a final state f via one, and only one, intermediate level m [9–11]. A convenient initial state is that formed in thermal or average resonance capture (ARC); the final state can be any low-lying discrete state. TSC spectra are determined by the branching ratios of the initial and intermediate states (expressed as ratios of partial to total widths Γ) and by the level density ρ of intermediate states with spin and parity J_m^π

$$I_{if}(E_1, E_2) = \sum_{XL, XL', J_m^\pi} \frac{\Gamma_{im}^{XL}(E_1)}{\Gamma_i} \rho(E_m, J_m^\pi) \frac{\Gamma_{mf}^{XL'}(E_2)}{\Gamma_m} + \sum_{XL, XL', J_{m'}^\pi} \frac{\Gamma_{im'}^{XL}(E_2)}{\Gamma_i} \rho(E_{m'}, J_{m'}^\pi) \frac{\Gamma_{m'f}^{XL'}(E_1)}{\Gamma_{m'}}. \quad (1)$$

The sums in Eq. (1) are restricted to give valid combinations of the level spins and parities and the transition multipolarities XL . They arise since one determines neither the ordering of the two γ rays, nor the multipolarities of the transitions nor the spins and parities of the intermediate levels, hence one has to include all possibilities. The two transition energies are correlated by $E_1 + E_2 = E_i - E_f$, thus, TSC spectra can be expressed as spectra of one transition energy E_γ only. TSC spectra are symmetric around $E_\gamma^{\text{sym}} = (E_i - E_f)/2$; integration over E_γ yields twice the total TSC intensity I_{if} (if both γ rays are counted in the spectrum). The knowledge of the parities π_i^1 and π_f ensures that I_{if} depends roughly speaking on the product of two RSFs around E_γ^{sym} [8] (i.e. $f_{E1}^2 + f_{M1}^2$ for $\pi_i = \pi_f$ and

¹ One assumes that only neutron s capture occurs.

$2f_{E1}f_{M1}$ for $\pi_i \neq \pi_f$, the latter case being more sensitive to the character of the soft resonance). I_{if} depends also on the level density. This usually prevents one to draw firm conclusions from TSC experiments alone [11]. A combined analysis of Oslo-type and TSC experiments, however, will enable one to establish the sum and product, respectively, of all contributions to f_{M1} and f_{E1} at energies of the soft resonance, thus determining its character. For this goal, the partial widths of Eq. (1) are expressed via

$$\Gamma_{x \rightarrow y}^{XL}(E_\gamma) = f_{XL}(E_\gamma) E_\gamma^{2L+1} D_x \quad (2)$$

in terms of RSFs and level spacings D_x . Eq. (2) actually gives only the average value of the Porter-Thomas distributed partial widths [12]. The total width Γ is the sum of all partial widths. Again, the sum is only the sum of mean values, however, the distribution of total widths with many components is almost δ -like [12]. The level density for a given spin and parity is calculated from the total level density by [13]

$$\rho(E_x, J_x^\pi) = \rho(E_x) \frac{1}{2} \frac{2J_x + 1}{2\sigma^2} \exp \left[-\frac{(J_x + 1/2)^2}{2\sigma^2} \right], \quad (3)$$

where σ is the spin cut-off parameter, and we assume equal numbers of positive and negative parity levels. This assumption and Eq. (3) have been verified from the discrete level schemes of rare earth nuclei. Thus, all quantities for calculating TSC spectra are based on experimental data.

The combined analysis is applied to the nucleus ^{172}Yb which has been investigated by the $^{173}\text{Yb}(^3\text{He}, \alpha\gamma)^{172}\text{Yb}$ reaction in Oslo and by the $^{171}\text{Yb}(n, \gamma\gamma)^{172}\text{Yb}$ reaction at the Lujan Center of the Los Alamos Neutron Science Center (LANSCE). The Oslo data have been reported in [4, 5]. Thus, only a short summary is given. The experiment was performed using a 45-MeV ^3He beam on a metallic, enriched, self-supporting target. Ejectiles were detected and their energies were determined using particle telescopes at 45° . In coincidence with α particles, γ rays were detected in an array of NaI detectors. From the reaction kinematics, α energy is converted into E_x , and γ cascade spectra are constructed for a range of E_x bins. The γ spectra are unfolded [14] and the primary γ spectra are extracted using a subtraction method [15]. The spectra are deconvoluted into a level density and a total RSF by applying the Brink-Axel hypothesis [16]. The level density is normalized by comparison to discrete levels at low E_x and to the average neutron resonance spacing at B_n [4]. The RSF is normalized using the average total width of neutron resonances, and is decomposed into

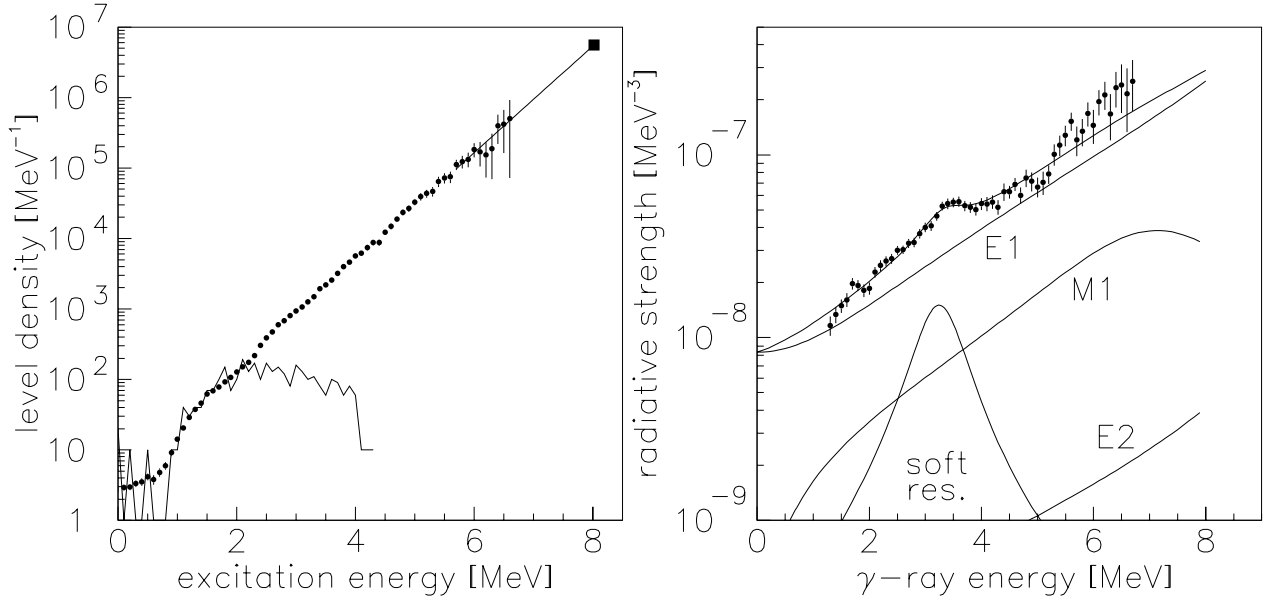


FIG. 1: Left panel: total level density (filled circles), constant-temperature extrapolation (solid line), level density at B_n derived from the average neutron resonance spacing (filled square) [7], and level density from counting of discrete levels (jagged line) [18]. Right panel: total RSF (filled circles), fit to the data, and decomposition into RSFs of different multiplicities (solid lines). The inclusion of the soft resonance in the fit decreases the χ^2_{red} from ~ 7.4 to ~ 1.3 . Since this value is close to unity, inclusion of additional non-statistical structures cannot significantly improve the fit.

the KMF $E1$ model, a spin-flip $M1$ model, and a soft dipole resonance [5]. Here, we have improved on the normalization of the level density and the RSF and included an isoscalar Lorentzian $E2$ model [17] giving

$$f_{\text{tot}} = K(f_{E1} + f_{M1}) + E_\gamma^2 f_{E2} + f_{\text{soft}}, \quad (4)$$

where K is a scaling factor of the order of one. Since quadrupole transitions populate levels within a broader spin interval than dipole transitions, Eq. (4) is of an approximative nature. Given the weakness of quadrupole transitions and the level of experimental uncertainties, however, this approximation is believed to be sufficient. The improved data, the fit to the total RSF, and its decomposition into different multiplicities are given in Fig. 1. The parameters for the $E1$ RSF are taken from [5], those for the $M1$ and $E2$ RSFs from [7], where

we use the f_{E1}/f_{M1} systematics at ~ 7 MeV giving values in agreement with ARC work [19]. The fit parameters are: the constant temperature of the KMF model $T = 0.34(3)$ MeV, the normalization coefficient $K = 1.7(1)$, and the three parameters of the soft resonance $E = 3.3(1)$ MeV, $\Gamma = 1.2(3)$ MeV, and $\sigma = 0.49(5)$ mb².

For the $^{171}\text{Yb}(n, \gamma\gamma)^{172}\text{Yb}$ experiment, we used ~ 1 g of enriched, dry Yb_2O_3 powder encapsulated in a glass ampoule, mounted in an evacuated beam tube and irradiated by collimated neutrons with a time-averaged flux of $\sim 4 \times 10^4$ neutrons/cm²s at ~ 20 m from the thermal moderator. γ rays were detected by two 80% and one shielded and segmented $\sim 200\%$ clover Ge(HP) detector, placed at ~ 12 cm from the target in a geometry to minimize angular correlation effects and contributions from higher multiplicity cascades. Single and coincident γ rays were recorded simultaneously, including n -time-of-flight and γ - γ coincidence time. The experiment ran for ~ 150 h yielding $\sim 10^7$ coincidences. The relative detector efficiencies from 1–9 MeV were determined by two separate runs of ~ 12 h each, before and after the $^{171}\text{Yb}(n, \gamma\gamma)^{172}\text{Yb}$ experiment, using the $^{35}\text{Cl}(n, \gamma)^{36}\text{Cl}$ reaction and its known γ intensities [20]. Also, a standard calibrated ^{60}Co source has been measured to adjust the relative curves to an absolute scale. The energy-summed coincidence spectrum (Fig. 2, upper panel) shows distinct peaks corresponding to TSCs between B_n and several low-lying states. The two strongest peaks have ~ 4000 counts each. TSC spectra (lower panels) were obtained by gating on three peaks, using the background subtraction method of [21] thereby avoiding spurious structures. Relative intensities of primary versus secondary γ rays were determined from the singles spectra and are in agreement with Ref. [19]. Absolute intensities were determined by using new data on absolute secondary γ -ray intensities [22] and scaling primary intensities to these values using the relative intensities of [19]. These absolute intensities are $\sim 20\%$ higher than in [19]. TSC intensities are normalized to (i) absolute primary intensities and secondary branching ratios of individual TSCs and (ii) by effectively estimating the number of neutron captures during the experiment from singles spectra, absolute (secondary) intensities, and absolute detector efficiencies. Both methods give equal results to within 10%.

TSC spectra are compared to calculations according to Eq. (1) assuming either electric

² The cited parameters are mean values obtained from the $^{173}\text{Yb}(^3\text{He}, \alpha\gamma)^{172}\text{Yb}$ and $^{172}\text{Yb}(^3\text{He}, ^3\text{He}'\gamma)^{172}\text{Yb}$ reaction data.

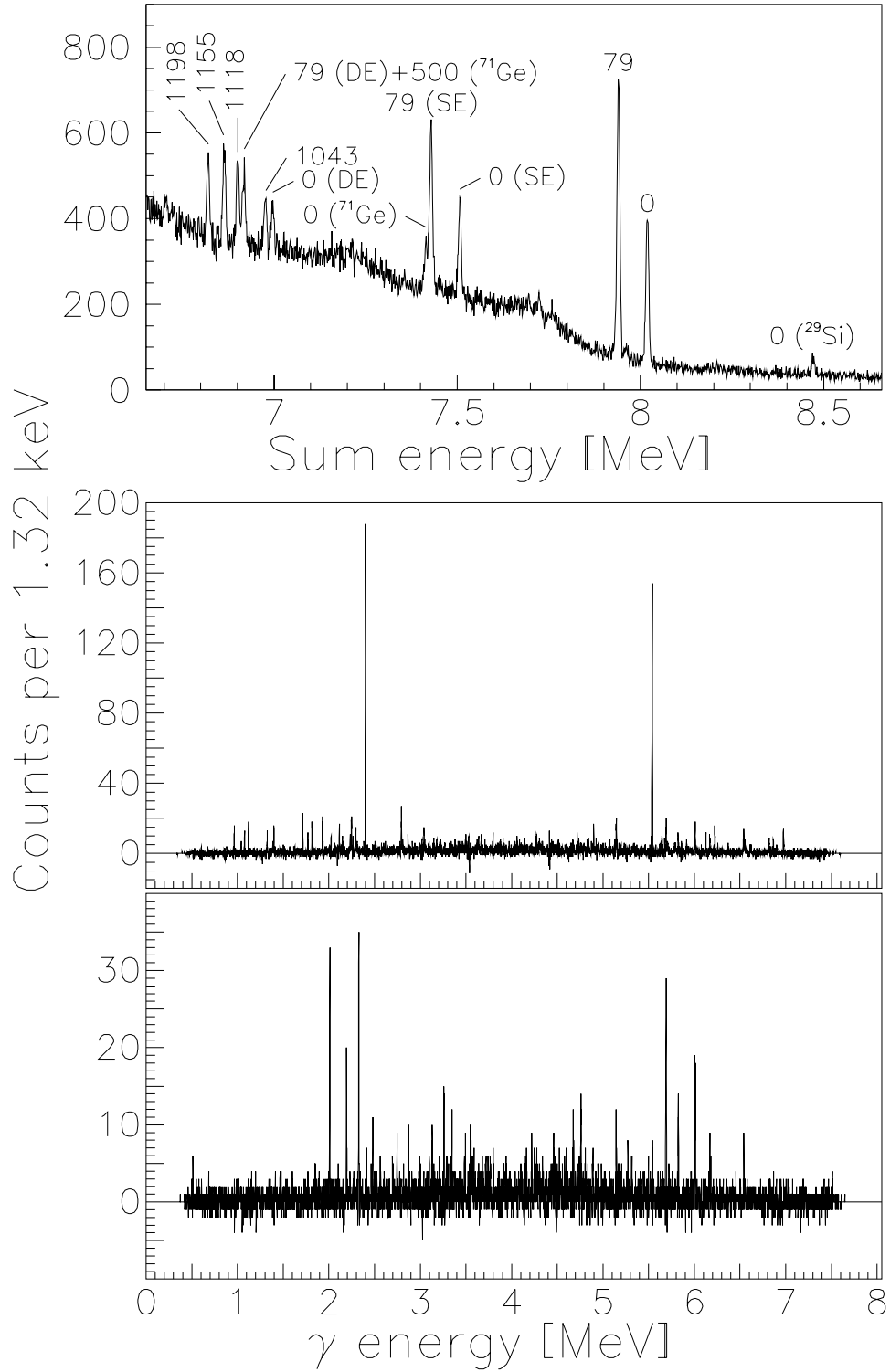


FIG. 2: Upper panel: energy-summed coincidence spectrum from the $^{171}\text{Yb}(n, \gamma)^{172}\text{Yb}$ reaction. The peaks are labeled by energy of the final state. Those denoted by ^{71}Ge and ^{29}Si are due to n -capture in the detector and in the glass ampoule, respectively. SE and DE stands for single and double escape peaks, respectively. TSC spectra to the 2_1^+ state at 79 keV (middle panel) and the 0_1^+ state at 0 keV (lower panel). The slight asymmetry is due to the energy-dependent resolution of the detectors.

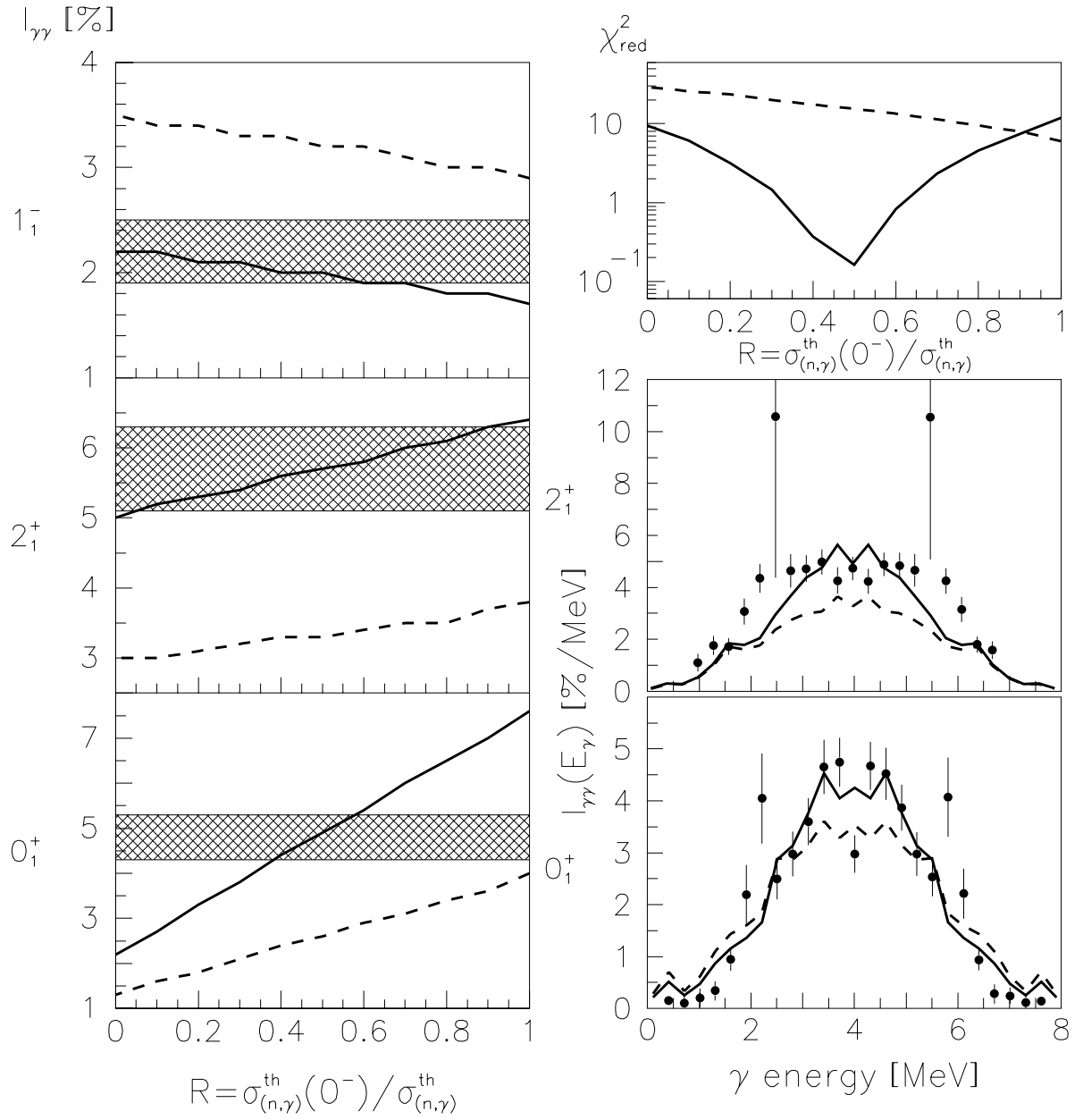


FIG. 3: Left: experimental values (hatched areas) for TSC intensities to final states 1_1^- at 1155 keV (upper panel), 2_1^+ (middle panel), and 0_1^+ (lower panel) compared to calculations as function of R . Solid and dashed lines correspond to the $M1$ and $E1$ hypotheses for the soft resonance. Right: combined χ_{red}^2 for all three TSC intensities as function of R for the $M1$ and $E1$ hypotheses (upper panel). Experimental (filled circles) and calculated TSC spectra to the 2_1^+ state (middle panel) and 0_1^+ state (lower panel) for the $M1$ hypothesis at $R = 0.5$ and the $E1$ hypothesis at $R = 1$. On the edges of the experimental spectra, the influence of Porter-Thomas fluctuations becomes visible.

or magnetic character for the soft resonance [8]. Due to the large Porter-Thomas fluctuations of TSC intensities, TSC spectra are compressed to 300 keV energy bins and only a 2.5 MeV broad energy interval in the middle of the spectra is taken into account [11] for the comparison. Corrections due to non-isotropic angular correlations of TSCs have been applied. They can be up to $\sim 20\%$, depending on the initial and final spins and parities involved in the respective TSCs. The contributions to the thermal radiative neutron capture cross section $\sigma_{n,\gamma}^{\text{th}}$ from the two possible spins (0^- and 1^-) involved in neutron s -capture on ^{171}Yb are uncertain. The compilation [23] assumes 0^- for the sub-threshold resonances which contribute 88% to $\sigma_{n,\gamma}^{\text{th}}$. Another 4% comes from 0^- resonances above threshold, giving in total a 92% contribution of 0^- states. On the other hand, there is no strong evidence that all contributing sub-threshold resonances have 0^- . Examination of hard primary γ -rays [19, 24] reveals many strong transitions populating 2^+ levels, indicating that a sizeable portion of $\sigma_{n,\gamma}^{\text{th}}$ stems from 1^- resonances. Therefore, we performed calculations for a set of ratios $R = \sigma_{n,\gamma}^{\text{th}}(0^-)/\sigma_{n,\gamma}^{\text{th}}$. These calculations show, however, that only the TSC intensity to the 0_1^+ state has a strong dependence on this ratio. Total experimental and calculated TSC intensities are shown in the left panels of Fig. 3. The calculations assuming $E1$ for the soft resonance do not reproduce the experimental intensities for any value of R . Good agreement is achieved assuming $M1$, with the additional condition of $R \sim 0.5$ for the 0_1^+ final state. However, it has to be emphasized that the conclusion of an $M1$ multipolarity for the soft resonance can be established from the TSC intensities to the 2_1^+ state and the 1_1^- state independently, irrespective of the value of R . Possible systematic uncertainties in the absolute normalization cannot change this conclusion, since in the case of the final states 0_1^+ and 2_1^+ , one would need a *decrease* while at the same time, for the 1_1^- final state one would need an *increase* in the experimental TSC intensities in order to accommodate the $E1$ hypothesis. The combined χ_{red}^2 for all three TSC intensities as function of R is also given. The $M1$ hypothesis yields the global minimum for $R = 0.5 \pm 0.2$ with $\chi_{\text{red}}^2 < 1$ whereas the minimal χ_{red}^2 for the $E1$ hypothesis is ~ 6 for $R = 1$. Finally, we show the TSC spectra to two final states compared to calculations using the $M1$ hypothesis at $R = 0.5$ and the $E1$ hypothesis at $R = 1$. No further conclusions have been drawn from this comparison, however.

The integrated strength of the soft resonance is expressed as

$$B^\uparrow(M1) = \frac{9\hbar c}{32\pi^2} \left(\frac{\sigma\Gamma}{E} \right)_{\text{soft}} \quad (5)$$

giving a value of $6.5(15) \mu_N^2$ which is entirely determined from the Oslo-type experiment after $M1$ multipolarity has been established. This is in agreement with the sum-rule approach for soft, orbital $M1$ strength [25] but is more than twice the strength from nuclear resonance fluorescence (NRF) [26]. However, in [11, 27] several limitations in determining $B^\uparrow(M1)$ using NRF are discussed, all resulting in possible underestimation. Concerns are that (i) too few 1^+ levels are observed in NRF experiments compared to level density estimates (eight candidates for 1^+ levels have been observed in the NRF experiment within the 2–4 MeV energy interval whereas ~ 120 such levels are expected from experimental level densities), (ii) the assumption in NRF experiments is not fulfilled that the total radiative width is given by the sum of the partial radiative widths for transitions to the ground state and the first excited state only, and (iii) the energy-region coverage is insufficient. Hence, in NRF experiments, weak, unobserved excitations from the ground state, weak, unobserved decays to excited levels above the ground-state rotational band, and excitations outside the investigated energy range might all contribute to an increased, summed $B^\uparrow(M1)$ value in better agreement with the present value [27]. Also in [11] $B^\uparrow(M1) \sim 7\mu_N^2$ is required in order to reproduce TSC spectra in ^{163}Dy .

In order to investigate the above mentioned concerns and to better compare the present result with the NRF observations, we have performed a simulation of the $^{172}\text{Yb}(\gamma, \gamma')$ experiment on the basis of the statistical model. The main assumption of this approach is that the mean value of partial radiative widths does not depend on concrete initial and final nuclear levels, but that it is determined by global nuclear characteristics such as the RSF and the level density. Each individual radiative width is, according to the statistical model, randomly distributed around this mean value and the probability for having any specific value is given by the Porter-Thomas distribution. The main observable in NRF experiments is the energy-integrated cross-section I_{0+1} of resonantly scattered γ rays populating an intermediate state at excitation energy E and then decaying down to either the ground state or the first excited state. This partial, energy-integrated, photo-absorption cross-section is given by

$$I_{0+1} = \frac{3\pi^2\hbar^2 c^2}{E^2} \frac{\Gamma_0 (\Gamma_0 + \Gamma_1)}{\Gamma}. \quad (6)$$

Here, Γ_0 and Γ_1 are the partial decay widths to the ground state and first excited state, respectively, and Γ is the total radiative width of the intermediate state with energy E . Similar partial cross-sections to higher-lying final states f can be calculated by replacing $\Gamma_0 + \Gamma_1$ with the appropriate Γ_f .

The information from the $^{172}\text{Yb}(\gamma, \gamma')$ experiment consists of the energies E and the partial, energy-integrated, photon-absorption cross-sections I_{0+1} of eight candidates for 1^+ states and of thirteen 1^- states [26]. Under the assumption that $\Gamma = \Gamma_0 + \Gamma_1$ and that all candidates for 1^+ states are, in fact, 1^+ states, the authors of [26] have deduced a summed $B^\dagger(M1)$ value for all eight candidate states of $2.4(10)\mu_N^2$.

Since, within the statistical model, the mean values of radiative widths can be expressed in terms of level densities and RSFs according to Eq. (2), we can use experimental values of these quantities from Oslo-type experiments to simulate a random set of NRF observable using Eq. (6). In order to properly take into account the detection threshold in NRF experiments, partial radiative widths for all possible γ transitions connecting intermediate 1^+ states with final states by dipole or quadrupole radiation have been simulated as random, Porter-Thomas distributed values with mean values determined by Eq. (2). Each set of simulated radiative widths has been used to calculate the partial, energy-integrated, photon-absorption cross-sections I_{0+1} for 1^+ states. The energy dependence of the detection threshold has been introduced according to [28]. Here, we would like to point out that the estimated energy dependence of the detection threshold in NRF experiments is only valid for the cases where the scattered γ ray has roughly the same energy as the incoming γ ray. Due to the $\sim 1/E_\gamma$ shape of the bremsstrahlung spectrum typically used in NRF investigations and the presence of non-resonantly scattered γ rays the experimental γ background for low-energy decays to excited states above the ground-state rotational band can be substantially higher. It is thus difficult to adjust the absolute scale of the detection threshold for different experiments due to a lack of information. Therefore, we have scaled the detection threshold in the simulation such that we observe, in average, eight levels above threshold in the energy range of 2–4 MeV. We have performed a total of 100 simulations from which summed mean values of partial, energy-integrated, photon-absorption cross-sections I_{0+1} are obtained.

Without taking into account the detection threshold, the simulation yields a mean value of integrated cross section for the sum of all 1^+ excitations in the energy region 2–4 MeV of ~ 0.8 MeV mb. If one takes into account only the eight levels above threshold, this

value reduces to $0.30(9)$ MeV mb. This value can be translated into $B^\dagger(M1) = 2.6(8) \mu_N^2$ which is in good agreement with the reported value of $B^\dagger(M1) = 2.4(10) \mu_N^2$ from NRF experiments. The remaining $M1$ strength is hidden in the background according to our simulation. Calculations also show that the assumption made in NRF experiments $\Gamma_0 + \Gamma_1 = \Gamma$ is only fulfilled for states with large values of I_{0+1} (i.e. transitions above threshold). This is in good agreement with [31] where the lifetimes of the most strongly populated 1^+ states in $^{162,164}\text{Dy}$ have been measured independently by inelastic neutron scattering. It turns out that there exists a strong positive correlation between I_{0+1} and $(\Gamma_0 + \Gamma_1)/\Gamma$, indicating that decay branches to higher-lying states become more important the weaker the state is populated to begin with. This result of the simulation could probably be tested experimentally at the quasi monoenergetic, 100% polarized High Intensity Gamma Source (HIGS) at the Duke University Free Electron Laser Laboratory and Triangle Universities Nuclear Laboratory.

In conclusion, the soft resonance found in the RSF of ^{172}Yb in Oslo-type experiments has been determined to be of $M1$ multipolarity by an auxiliary TSC measurement. The strength of the $M1$ resonance is $B^\dagger(M1) = 6.5(15) \mu_N^2$ which is entirely determined by the former experiment. This value agrees with a sum-rule approach for orbital strength, but is more than twice the value reported by NRF experiments. However, this difference can be explained tentatively on the basis of the statistical model. Our simulation hints that a possible source for underestimation of $B^\dagger(M1)$ strength in NRF experiments can arise from weakly excited states and weak decays to excited states above the ground-state rotational band. Those weak transitions might be missed in NRF experiments due to the presence of an experimental detection thresholds. Additional experimental data to resolve this question are highly desirable. Assuming $M1$ multipolarity for similar soft resonances in other rare earth nuclei gives consistent strengths of $\sim 6 \mu_N^2$ for various even and odd Dy, Er, and Yb nuclei and quenched strengths of $\sim 3 \mu_N^2$ for the more spherical Sm nuclei [32]. The centroids of the resonances increase weakly with mass number.

This work has benefited from the use of the Los Alamos Neutron Science Center at the Los Alamos National Laboratory. This facility is funded by the U.S. Department of Energy under Contract W-7405-ENG-36. Part of this work was performed under the auspices of the U.S. Department of Energy by the University of California, Lawrence Livermore National Laboratory under Contract W-7405-ENG-48, and Los Alamos National Laboratory under Contract W-7405-ENG-36. Financial support from the Norwegian Research Council (NFR)

is gratefully acknowledged. A.V. acknowledges support from a NATO Science Fellowship under project number 150027/432. E.A. acknowledges support by U.S. Department of Energy Grant No. DE-FG02-97-ER41042. We would like to thank Gail F. Eaton for making the targets.

-
- [1] G.A. Bartholomew *et al.*, Adv. Nucl. Phys. **7**, 229 (1973).
 - [2] Samuel S. Dietrich and Barry B. Berman, At. Data Nucl. Data Tables **38**, 199 (1988).
 - [3] J. Kopecky and M. Uhl, in Proceedings of a Specialists' Meeting on Measurement, Calculation and Evaluation of Photon Production Data, Bologna, Italy, 1994, Report No. NEA/NSC/DOC(95)1, p. 119.
 - [4] A. Schiller *et al.*, Nucl. Instrum. Methods Phys. Res. A **447**, 498 (2000).
 - [5] A. Voinov *et al.*, Phys. Rev. C **63**, 044313 (2001).
 - [6] S.G. Kadmskiĭ, V.P. Markushev, and V.I. Furman, Yad. Fiz. **37**, 277 (1983) [Sov. J. Nucl. Phys. **37**, 165 (1983)].
 - [7] *Handbook for Calculations of Nuclear Reaction Data* (IAEA, Vienna, 1998).
 - [8] A. Voinov *et al.*, Nucl. Instrum. Methods Phys. Res. A **497**, 350 (2003).
 - [9] A.M. Hoogenboom, Nucl. Instrum. Methods Phys. Res. **3**, 57 (1958).
 - [10] S.T. Boneva *et al.*, Fiz. Elem. Chastits At. Yadra **22**, 479, 1433 (1991) [Sov. J. Part. Nucl. **22**, 232, 698 (1991)].
 - [11] F. Bečvář *et al.*, Phys. Rev. C **52**, 1278 (1995).
 - [12] C.E. Porter and R.G. Thomas, Phys. Rev. **104**, 483 (1956).
 - [13] A. Gilbert and A.G.W. Cameron, Can. J. Phys. **43**, 1446 (1965).
 - [14] M. Guttormsen *et al.*, Nucl. Instrum. Methods Phys. Res. A **374**, 371 (1996).
 - [15] M. Guttormsen, T. Ramsøy, and J. Rekstad, Nucl. Instrum. Methods Phys. Res. A **255**, 518 (1987).
 - [16] D.M. Brink, Ph.D. thesis, Oxford University, 1955; P. Axel, Phys. Rev. **126**, 671 (1962).
 - [17] W.V. Prestwich, M.A. Islam, and T.J. Kennett, Z. Phys. A **315**, 103 (1984).
 - [18] R. Firestone and V.S. Shirley, *Table of Isotopes*, 8th ed. (Wiley, New York, 1996).
 - [19] R.C. Greenwood, C.W. Reich, and S.H. Vegors Jr., Nucl. Phys. **A252**, 260 (1975).
 - [20] C. Coceva, A. Brusegan, and C. van der Vorst, Nucl. Instrum. Methods Phys. Res. A **378**,

511 (1996).

- [21] E.V. Vasilieva *et al.*, Bull. Russ. Acad. Sci. Phys. **57**, 1549 (1993).
- [22] R. Firestone, private communication.
- [23] S.F. Mughabghab *Neutron Cross Sections*, (Academic Press, New York, 1984), Vol. I, part B.
- [24] W. Gelletly *et al.*, J. Phys. G **11**, 1055 (1985).
- [25] E. Lipparini and S. Stringari, Phys. Rep. **175**, 103 (1989).
- [26] A. Zilges *et al.*, Nucl. Phys. **A507**, 399 (1990); **A519**, 848 (1990).
- [27] A. Schiller *et al.*, preprint nucl-ex/0011018.
- [28] A. Nord *et al.*, Phys. Rev. C **96**, 2287 (1996).
- [29] J. Margraf *et al.*, Phys. Rev. C **52**, 2429 (1995).
- [30] H. Maser *et al.*, Phys. Rev. C **53**, 2749 (1996).
- [31] E.L. Johnson *et al.*, Phys. Rev. C **52**, 2382 (1995).
- [32] S. Siem *et al.*, Phys. Rev. C **65**, 044318 (2002).